

Received:  
14 April 2018

Revised:  
29 June 2018

Accepted:  
27 July 2018

<https://doi.org/10.1259/bjr.20180345>

Cite this article as:

Thompson SM, Garg I, Ehman EC, Sheedy SP, Bookwalter CA, Carter RE, et al. Non-alcoholic fatty liver disease-associated hepatocellular carcinoma: effect of hepatic steatosis on major hepatocellular carcinoma features at MRI. *Br J Radiol* 2018; **91**: 20180345.

## FULL PAPER

# Non-alcoholic fatty liver disease-associated hepatocellular carcinoma: effect of hepatic steatosis on major hepatocellular carcinoma features at MRI

<sup>1</sup>SCOTT M THOMPSON, MD, PhD, <sup>1</sup>ISHAN GARG, MBBS, <sup>1</sup>ERIC C EHMAN, MD, <sup>1</sup>SHANNON P SHEEDY, MD, <sup>1</sup>CANDICE A BOOKWALTER, MD, PhD, <sup>2</sup>RICKEY E CARTER, PhD, <sup>3</sup>LEWIS R ROBERTS, MBBS, PhD and <sup>1</sup>SUDHAKAR K VENKATESH, MD

<sup>1</sup>Department of Radiology, Mayo Clinic School of Medicine, Mayo Clinic, Rochester, MN, USA

<sup>2</sup>Division of Biomedical Statistics and Informatics, Mayo Clinic School of Medicine, Mayo Clinic, Jacksonville, FL, USA

<sup>3</sup>Division of Gastroenterology and Hepatology, Mayo Clinic School of Medicine, Mayo Clinic, Rochester, MN, USA

Address correspondence to: Dr Sudhakar K Venkatesh

E-mail: [venkatesh.sudhakar@mayo.edu](mailto:venkatesh.sudhakar@mayo.edu)

**Objective:** To evaluate the effect of hepatic steatosis on LI-RADS® major features at MRI in patients with non-alcoholic fatty liver disease (NAFLD)-associated hepatocellular carcinoma (HCC).

**Methods:** HCC and liver parenchyma features at MRI from 48 consecutive patients with NAFLD and histology proven HCC (mean ± SD; 4.5 ± 3.4 cm) were independently reviewed by three radiologists. Inter-rater agreement was determined by prevalence/bias-adjusted kappa. Hepatic fat signal fraction (FS%) was independently calculated. HCC features were compared by FS% at MRI using logistic regression analysis and histologic steatosis grade using Cochran-Armitage test for trend, stratified by cirrhotic liver morphology or histologic fibrosis stage. Receiver operating characteristic curves were generated to determine the sensitivity and specificity for major HCC features by FS%.

**Results:** Major HCC features included arterial phase hyperenhancement (APHE) in 45 (93%), portal venous phase washout (PVWO) in 30 (63%), delayed phase washout (DPWO) in 38 (79%) and enhancing “capsule” in 34 (71%). Cirrhotic morphology was present in 22

(46%). Inter-rater agreement was 0.75 for APHE, 0.42–0.58 for PVWO, 0.58–0.71 for DPWO and 0.38–0.67 for enhancing “capsule”. There was an 18%, 14% and 22% increase in the odds of absent PVWO, DPWO and capsule appearance for every 1% increase in hepatic FS% in patients with non-cirrhotic liver morphology ( $p = 0.011, 0.040$  and  $0.029$ , respectively). Hepatic FS%  $\geq 14.8\%$  had a sensitivity and specificity of 64 and 100% for absent PVWO and 71 and 90% for absent DPWO in patients with non-cirrhotic liver morphology.

**Conclusion:** Absent washout and capsule appearance are associated with increasing hepatic steatosis in patients with non-cirrhotic, NAFLD-associated HCC.

**Advances in knowledge:** In patients with non-cirrhotic, non-alcoholic fatty liver disease (NAFLD)-associated hepatocellular carcinoma (HCC), absent HCC washout and capsule appearance are associated with increasing hepatic steatosis, thereby potentially impacting the noninvasive imaging diagnosis of HCC in these patients. Lack of washout or capsule appearance in steatotic livers at MRI may require alternative criteria for the diagnosis of HCC in patients with non-cirrhotic NAFLD.

## INTRODUCTION

Hepatocellular carcinoma (HCC) is the second leading cause of cancer-related death worldwide with a rising incidence both in the United States and globally.<sup>1–3</sup> The predominant risk factor for HCC is hepatic cirrhosis, most commonly secondary to viral hepatitis B (HBV) or C (HCV) or alcoholic hepatitis.<sup>4–7</sup> In recent years, studies have identified an increased risk of developing HCC in patients with non-alcoholic fatty liver disease (NAFLD).<sup>8,9</sup> Of note, it is now estimated that 4–22% of HCC cases in Western countries can be attributed to NAFLD.<sup>2,10–15</sup> Data suggest that HCC in NAFLD may arise

in the absence of hepatic fibrosis or cirrhosis, thereby raising questions about which patients to screen for HCC when traditional risk factors are absent.<sup>3,16,17</sup> Diagnosis of NAFLD requires (i) evidence of hepatic steatosis (HS) by either histology or imaging, (ii) absence of competing etiologies for hepatic steatosis, (iii) no significant alcohol consumption and (iv) no co-existing etiologies for chronic liver disease.<sup>18</sup> Moreover, NAFLD is frequently associated with obesity and metabolic syndrome. With the rising incidence and prevalence of obesity, metabolic syndrome and NAFLD worldwide,

the incidence of HCC secondary to NAFLD is likely to continue to rise.<sup>19–22</sup>

HCC, unlike most malignancies, is unique given its characteristic imaging appearance and is most commonly diagnosed non-invasively by multiphase contrast-enhanced CT or MRI, thereby obviating the need for histologic confirmation.<sup>23–26</sup> The European Association for the Study of the Liver (EASL), European Organization for Research and Treatment of Cancer (EORTC) and American Association for the Study of Liver Diseases (AASLD) have developed guidelines for non-invasive imaging diagnosis of HCC based on specific imaging hallmarks of HCC in patients with cirrhosis.<sup>23,24,27</sup> Additionally, the Liver Imaging Reporting and Data System (LI-RADS) was developed to provide standardized reporting of imaging features in patients at risk for HCC including those with cirrhosis, chronic HBV infection or current or prior HCC.<sup>26,28,29</sup> However, CT/MRI LI-RADS® 2014 and current 2017 criteria (Supplementary Table 1) as well as EASL-EORTC and AASLD guidelines have not been validated in patients with NAFLD in whom histologic and/or imaging evidence of cirrhosis may be absent. In fact, studies on imaging characteristics of HCC in NAFLD are rare. Iannaccone *et al* reviewed CT and MRIs of HCCs in 22 patients with NAFLD and showed that these HCCs typically presented as a large solitary, encapsulated mass with arterial hyperenhancement in a non-cirrhotic liver.<sup>30</sup> However, it is not known if the degree of hepatic steatosis in NAFLD affects CT/MRI LI-RADS® major diagnostic imaging features including HCC arterial phase hyperenhancement (APHE), washout appearance, and enhancing “capsule”.<sup>26,28,31,32</sup> Moreover, while studies have examined interobserver agreement for HCC major features in cirrhotics, agreement has not yet been explored in the setting of NAFLD.<sup>33–35</sup>

The aim of this study was to evaluate the effect of hepatic steatosis on LI-RADS® major features at MRI in patients with NAFLD-associated HCC.

## METHODS AND MATERIALS

### Patient selection

After receiving approval from the Institutional Review Board and obtaining a waiver of informed consent, a HIPAA-compliant retrospective review was undertaken using the comprehensive electronic medical records of consecutive patients with NAFLD and pathology proven HCC from 1/1/2001 to 12/31/2016. Inclusion criteria included: (1) MRI of the liver included at least dynamic contrast-enhanced series and in- and opposed-phase sequence, (2) pathology proven HCC, (3) biopsy proven hepatic steatosis  $\geq 5\%$  and/or hepatic fat signal fraction  $\geq 5\%$  at MR imaging and (4) no competing aetiology for hepatic steatosis and (5) no coexisting causes of chronic liver disease or alcoholic liver disease.<sup>18</sup> A total of 90 patients with a diagnosis of NAFLD and pathology proven HCC were identified during the indicated time period. Of the 90 patients identified, 42 patients were excluded due to coexisting chronic hepatitis B (HBV) or chronic hepatitis C (HCV) infection, alcoholic liver disease and/or hereditary hemochromatosis ( $N = 42$ ). Ultimately, 48 patients formed the final study group. The NAFLD disease spectrum was defined based

on American Association for the Study of Liver Diseases categories: non-alcoholic fatty liver (NAFL) with hepatic steatosis  $\geq 5\%$  and no evidence of hepatocellular injury or fibrosis; non-alcoholic steatohepatitis (NASH) with hepatic steatosis  $\geq 5\%$  and with inflammation  $\pm$  fibrosis; NASH cirrhosis, cirrhosis with current or past evidence of steatosis or steatohepatitis; and cryptogenic cirrhosis, cirrhosis with no obvious aetiology and with metabolic risk factors such as obesity and metabolic syndrome.<sup>18</sup>

### Multireader MRI review

MRI HCC features and liver parenchyma characteristics were independently reviewed by three board-certified abdominal radiologists with 3, 10 and 15 years of experience in abdominal imaging (Author X, Y, Z). Final MRI features were determined by majority. HCC features evaluated included arterial phase hyperenhancement (APHE), portal venous phase washout (PVWO), delayed phase washout (DPWO), presence of an enhancing “capsule” and  $T_2$  weighted ( $T_2W$ ),  $T_1$  weighted ( $T_1W$ ) and diffusion (DWI) signal intensity. All sequences were available in all patients except for DWI, which was available in only 32 of 48 patients. Gadolinium based extracellular contrast medium (Gadoterate meglumine, DOTAREM® Guerbert LLC or gadobutrol, GADAVIST® Bayer Healthcare) was used for contrast enhanced sequences in this study. Digital subtraction was not used routinely to assess post contrast images. Readers assessed for enhancing “capsule” in the portal venous and delayed phases of contrast enhancement. In patients with multiple HCCs, the MRI features of the largest HCC with histologic confirmation were evaluated. Cirrhotic liver morphology was graded as present or absent based on the subjective assessment of surface nodularity, right hepatic lobe liver atrophy, left lobe hypertrophy, caudate lobe hypertrophy and widened fissures, as well as on secondary signs of portal hypertension including splenomegaly, ascites and portosystemic venous collaterals.

### Fat signal fraction (FS%) calculation

Hepatic fat signal fraction (FS%) was determined by an independent observer blinded to histological grade of steatosis using a previously described method.<sup>36</sup> The largest possible region of interest (ROI) was drawn at a single slice location on the non-tumor bearing liver parenchyma in the posterior right hepatic lobe on the in- and opposed phase images while avoiding major vascular structures and artefact. Hepatic fat signal fraction was calculated as  $[(S_{IP} - S_{OP}) / 2 * S_{IP}]$  where  $S_{IP}$  is the mean signal on in phase images while  $S_{OP}$  is the mean signal observed on opposed phase images.

### Tumor pathology review

HCC tumor grade (well, well-moderately, moderately, moderately-poorly and poorly differentiated types), hepatic histologic steatosis grade (none ( $< 5\%$ ), mild (5–33%), moderate, (33–66%), severe ( $> 66\%$ )) and hepatic fibrosis stage (0, 1, 2, 3, 4) were extracted from official pathology reports.

### Statistical methods

Data were analyzed using JMP 13.0 (SAS, Cary, NC) and Prism 7.0 (GraphPad Software, Inc, La Jolla, CA). Descriptive statistics were generated with continuous variables presented as

mean  $\pm$  standard deviation and/or median—interquartile range (IQR—25th to 75th percentile) and categorical variables as counts (proportions). Inter-rater agreement was determined by prevalence-adjusted bias-adjusted Cohen's kappa<sup>37</sup> to account for the imbalanced ratio of HCCs with APHE to no APHE and  $T_2W$  hyperintensity to no  $T_2W$  hyperintensity. Agreement between cirrhotic liver morphology by MRI and histologic cirrhosis was determined by prevalence-adjusted Cohen's kappa.<sup>37</sup> Differences between non-cirrhotic and cirrhotic sub groups were compared using an unpaired t-test with equal variance assumption for continuous data and Fisher's exact test for categorical data. Hepatic FS% was compared by histologic steatosis grade using Kruskal-Wallis test. HCC features were compared by hepatic FS% stratified by cirrhotic liver morphology at MRI or histologic fibrosis stage using logistic regression and the unit odds ratio (OR) and 95% confidence interval (CI) for every 1% increase in hepatic FS% calculated. HCC features were compared by histologic steatosis grade (mild, moderate, severe) stratified by cirrhotic liver morphology at MRI or histologic fibrosis stage using Cochran-Armitage test for trend. Receiver operating characteristic (ROC) curves were generated to determine the area under the curve (AUC) and the sensitivity and specificity at different cutoffs for hepatic FS% in differentiating absent portal venous and delayed phase washout and enhancing capsule appearance. Two-sided  $p < .05$  was considered statistically significant. All  $p$ -values reported are raw  $p$ -values that have not been inflated to account for multiple testing correction.

## RESULTS

### Patient, HCC and liver parenchyma characteristics by liver morphology

48 patients were identified who had NAFLD and pathologically confirmed HCC (Figure 1 for study flow diagram). Demographic, clinical, imaging and pathology data are

summarized in Table 1. 26 patients had non-cirrhotic liver morphology (54.2%) and 22 patients had cirrhotic liver morphology (45.8%) at MRI. Patients with cirrhotic liver morphology had higher proportion of diabetes compared to patients with non-cirrhotic liver morphology (86% v. 31%;  $p < 0.001$ ).

The mean  $\pm$  SD HCC tumor size (cm) was  $4.5 \pm 3.4$  cm and was significantly larger in patients with non-cirrhotic versus cirrhotic liver morphology ( $5.7 \pm 3.4$  v.  $3.3 \pm 3.0$  cm;  $p = 0.014$ ). The mean  $\pm$  SD hepatic fat signal fraction (FS%) by MRI was  $8.0 \pm 8.4\%$  with a trend toward decreased hepatic FS% in patients with cirrhotic versus non-cirrhotic liver morphology ( $5.9 \pm 8.1\%$  v.  $9.7 \pm 8.4\%$ , respectively;  $p = 0.12$ ). Assessment of HCC features and liver parenchyma morphology by majority consensus and by individual reader are reported in Table 2 and Supplemental Table 2. Patients with cirrhotic liver morphology had a significantly lower proportion of HCCs with  $T_2W$  hyperintensity (63% v. 100%;  $p < 0.001$ ),  $T_1$  hypointensity (23% vs 89%;  $p < 0.001$ ) and DWI hyperintensity (69% vs 100%;  $p = 0.019$ ) compared to patients with non-cirrhotic liver morphology (Supplementary Figure 1).

### HCC features and liver morphology—Inter-rater agreement

Inter-rater agreement for HCC features and for cirrhotic liver morphology for the entire cohort are reported in Table 3. Inter-rater agreement for HCC features stratified by cirrhotic liver morphology is reported in Supplemental Table 3. Agreement between cirrhotic liver morphology at MRI and histologic fibrosis Stage 3–4 at pathology was good (kappa = 0.75).

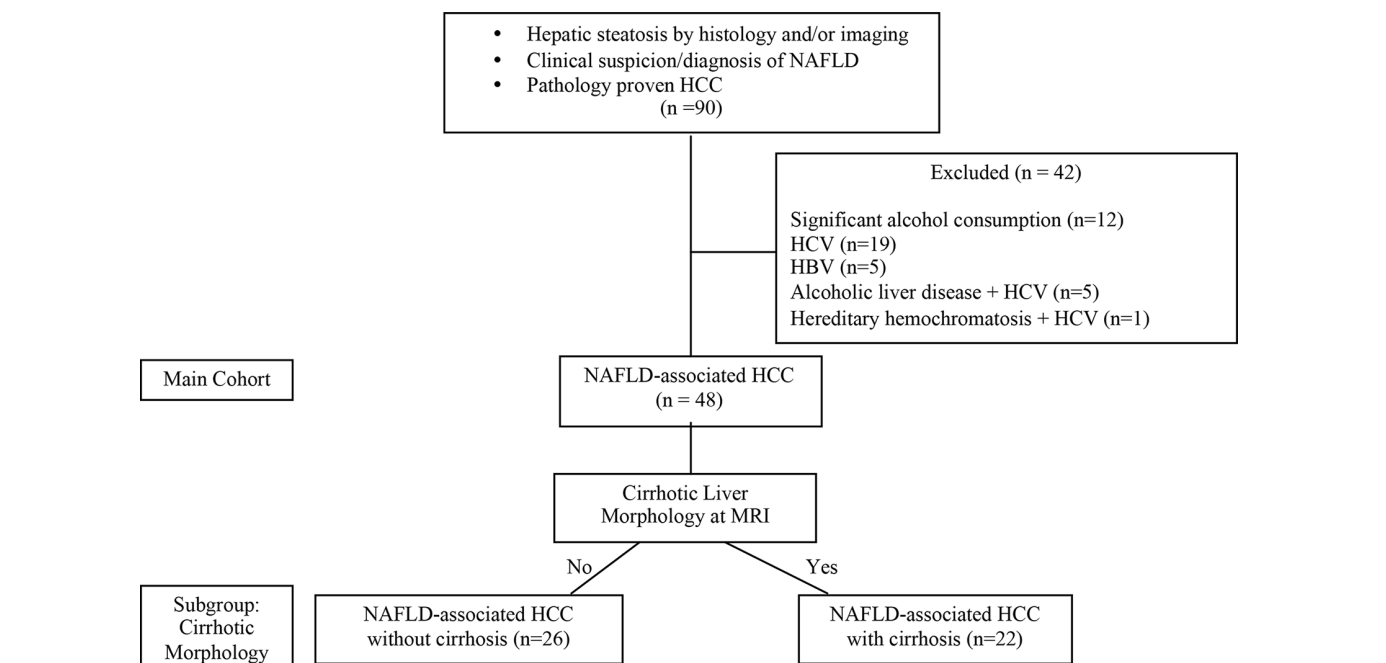


Table 1. Demographic, clinical, imaging and pathology data in patients with NAFLD-associated HCC (*n* = 48; main) by non-cirrhotic (*n* = 26) and cirrhotic (*n* = 22) liver morphology

	Main Cohort ( <i>n</i> = 48)	Non-cirrhotic morphology ( <i>n</i> = 26)	Cirrhotic morphology ( <i>n</i> = 22)	<i>p</i> -value
Age (years) (mean ± SD) (IQR)	64.6 ± 9.9 (60.7 to 73.5)	67.3 ± 8.8 (60.7 to 68.0)	61.4 ± 10.3 (56.4 to 68.3)	0.042
Gender				0.53
Female	13 (27.1)	6 (23.0)	7 (31.8)	
Male	35 (72.9)	20 (76.9)	15 (68.2)	
BMI (kg m <sup>-2</sup> ) (mean ± SD) (IQR)	32.5 ± 5.4 (29.5 to 34.6)	32.4 ± 5.0 (29.5 to 34.6)	32.7 ± 6.1 (27.6 to 38.0)	0.84
Diabetes (%)	27 (56.2)	8 (30.8)	19 (86.4)	<0.001
Total cholesterol (mean ± SD)(IQR)	175 ± 61 (149 to 204)	182 ± 52 (149 to 204)	169. ± 70 (125 to 192)	0.53
Triglycerides (mean ± SD) (IQR)	141 ± 76 (116 to 206)	165 ± 93 (116 to 206)	116 ± 43 (86 to 132)	0.044
Hepatic steatosis diagnosis				1.0
Biopsy	47 (98.0)	26 (100)	21 (95.5)	
Imaging (FS ≥ 5%)	1 (2.0)	0 (0)	1 (4.5)	
Tumor size (cm) mean ± SD (IQR)	4.5 ± 3.4 (3.5 to 6.7)	5.7 ± 3.4 (3.5 to 6.7)	3.3 ± 3.0 (2.0 to 3.4)	0.014
Hepatic fat signal fraction (FS%) mean ± SD (IQR)	8.0 ± 8.4 (2.8 to 15.4)	9.7 ± 8.4 (2.8 to 15.4)	5.9 ± 8.1 (1.6 to 8.6)	0.12
HCC pathology source				
Biopsy	6 (12.5)	2 (7.7)	4 (18.2)	
Surgical resection	30 (62.5)	24 (92.3)	6 (27.3)	
Liver explant at transplant	12 (25.0)	0 (0)	12 (54.5)	
Pathologic features				
Tumor grade				0.23
Well differentiated	12 (25.0)	6 (23.1)	6 (27.2)	
Well-moderately differentiated	1 (2.1)	0 (0)	1 (4.5)	
Moderately differentiated	28 (58.3)	14 (53.8)	14 (63.6)	
Moderately poor differentiated	7 (14.6)	6 (23.1)	1 (4.5)	
Hepatic steatosis grade				0.75
None	0 (0)	0 (0)	0 (0)	
Mild	39 (81.3)	20 (77.0)	19 (86.4)	
Moderate	5 (10.4)	3 (11.5)	2 (9.1)	
Severe	4 (8.3)	3 (11.5)	1 (4.5)	
Hepatic fibrosis stage				<0.001
0	12 (25.0)	10 (38.5)	2 (9.1)	
1	9 (18.8)	8 (30.8)	1 (4.5)	
2	5 (10.4)	5 (19.2)	0 (0)	
3	4 (8.3)	1 (3.8)	3 (13.4)	
4	18 (37.5)	2 (7.7)	16 (72.7)	

BMI, body mass index; HCC, hepato cellular carcinoma; IQR, interquartile range (25th to 75th percentile).

*p*-value for non-cirrhotic group versus cirrhotic group; continuous variables analyzed using unpaired *t*-test with equal variance assumption; categorical data analyzed using Fisher's exact test.

#### Hepatic fat signal fraction (FS%) by histologic steatosis grade

Median (IQR) FS% increased by histologic steatosis grade: 3.6% (1.8 to 9.2) (mild), 12.5% (7.6 to 15.8) (moderate) and 20.4% (16.4 to 26.8) (severe) (*p* = 0.003) (Figure 2).

#### HCC features at MRI by hepatic fat signal fraction (FS%)

Absent PVWO, DPWO and enhancing capsule appearance were significantly associated with increasing hepatic FS% among patients with non-cirrhotic liver morphology with an 18%,

Table 2. HCC features and liver parenchyma morphology at MRI by majority consensus in patients with NAFLD-associated HCC (n = 48) by non-cirrhotic (n = 26) and cirrhotic (n = 22) liver morphology

HCC imaging features	Main cohort (n = 48)	Non-cirrhotic morphology (n = 26)	Cirrhotic morphology (n = 22)	p-value
APHE	45 (93.4)	24 (92.3)	21 (95.4)	1.0
PVWO	30 (62.5)	15 (57.7)	15 (68.1)	0.56
DPWO	38 (79.2)	19 (73.1)	19 (86.3)	0.31
Enhancing "Capsule"	34 (70.8)	21 (80.1)	13 (59.1)	0.12
T <sub>2</sub> W hyperintense	40 (83.3)	26 (100)	14 (63.4)	<0.001
T <sub>1</sub> W hypointense	28 (58.3)	23 (88.5)	5 (22.7)	<0.001
DWI hyperintense	*28 (87.5)	**19 (100)	***9 (69.2)	0.019

APHE, arterial phase hyperenhancement; DPWO, delayed phase washout; DWI, diffusion weighted imaging; T<sub>1</sub>W, T<sub>1</sub> weighted; T<sub>2</sub>W, T<sub>2</sub> weighted. DWI available for \*32/48, \*\*19/26 and \*\*\* 13/22. p-value for non-cirrhotic group versus cirrhotic group; categorical data analyzed using Fisher's exact test.

14% and 22% increase in the odds of absent PVWO, DPWO and enhancing capsule for every 1% increase in hepatic FS% (p = 0.011, 0.040 and 0.029, respectively) (Table 4; Figures 3 and 4). Absent PVWO was also associated with increasing hepatic FS% among patients with lower histologic fibrosis stage (0 to 2) with a 13% increase in the odds of absent PVWO for every 1% increase in hepatic FS% (Supplementary Table 4; p = 0.033). There was no association between absent major HCC features and increasing hepatic FS% among patients with cirrhotic liver morphology (Table 4; Figure 5) or higher histologic fibrosis stage<sup>3,4</sup> (Supplementary Table 4).

HCC features at MRI by histologic steatosis grade  
Absent DPWO and enhancing capsule appearance were significantly associated with increasing histologic steatosis grade among patients with non-cirrhotic liver morphology (p = 0.003 and 0.016, respectively) but not cirrhotic liver morphology (p = 0.56 and p = 0.57, respectively) (Figure 6; Supplementary Table 5). Similarly, absent PVWO, DPWO and enhancing capsule

appearance were associated with increasing histologic steatosis grade among patients with hepatic fibrosis stage 0–2 (p = 0.018, <0.001 and p = 0.016, respectively) but not hepatic fibrosis Stage 3–4 (p = 0.57, p = 0.92, p = 0.57 respectively) (Supplementary Figure 2 and Supplementary Table 5).

Receiver Operating Characteristic (ROC) analysis: HCC washout and capsule by hepatic FS% among patients with non-cirrhotic liver morphology  
The areas under the receiver-operating characteristic (ROC) curve for absent PVWO, DPWO and enhancing capsule appearance by hepatic FS% among patients without cirrhotic liver morphology were good (0.83, 0.83 and 0.81, respectively; Figure 7). A hepatic FS% cutoff of >14.8% had a sensitivity and specificity of 64 and 100% for absent PVWO and 71 and 90% for absent DPWO, respectively. A hepatic FS% cutoff of ≥18.6% had

Table 3. Interobserver agreement for HCC features and liver parenchyma morphology at MRI in patients with NAFLD-associated HCC (n = 48)

HCC imaging features	R1 vs R2	R1 vs R3	R2 vs R3
APHE	0.75	0.75	0.75
PVWO	0.42	0.50	0.58
DPWO	0.58	0.71	0.71
Enhancing "Capsule"	0.46	0.38	0.67
T <sub>2</sub> W signal	0.88	0.83	0.79
T <sub>1</sub> W signal	0.58	0.63	0.75
DWI signal*	0.58	0.53	0.70
Cirrhotic liver morphology	0.63	0.54	0.50

APHE, arterial phase hyper enhancement; DPWO, delayed phase washout; DWI, diffusion-weighted imaging; PVWO, portal venous phase washout; R1, reader 1; R2, reader 2; R3, reader 3; T<sub>1</sub>W, T<sub>1</sub> weighted; T<sub>2</sub>W, T<sub>2</sub> weighted.

Data are presented as prevalence-adjusted bias-adjusted kappa.

Figure 2. Hepatic signal fraction (FS%) by histologic steatosis grade (mild, moderate and severe). Data are presented as median (IQR) and analyzed using Kruskal-Wallis test. IQR, inter quartile range.

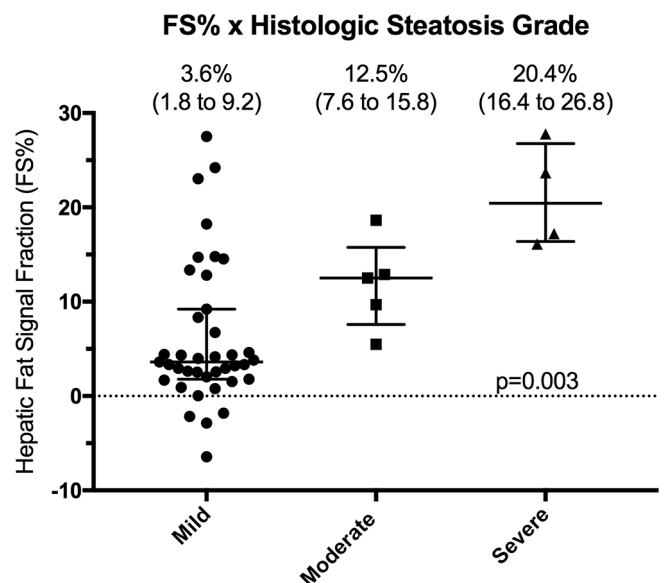


Table 4. HCC features at MRI by hepatic fat signal fraction (FS%) in patients with NAFLD-associated HCC ( $n = 48$ ; main) by non-cirrhotic ( $n = 26$ ) and cirrhotic ( $n = 22$ ) liver morphology

HCC imaging feature	Main Cohort ( $n = 48$ )			Non-cirrhotic morphology ( $n = 26$ )			Cirrhotic morphology ( $n = 22$ )		
	Unit OR	95% CI	$p$ -value	Unit OR	95% CI	$p$ -value	Unit OR	95% CI	$p$ -value
APHE present	1.19	0.91 to 1.54	0.20	1.30	0.80 to 2.13	0.29	1.16	0.76 to 1.79	0.49
PVWO absent	1.05	0.98 to 1.13	0.18	1.18	1.04 to 1.36	0.011	0.88	0.73 to 1.06	0.18
DPWO absent	1.06	0.98 to 1.15	0.17	1.14	1.01 to 1.29	0.040	0.85	0.64 to 1.12	0.25
Enhancing “Capsule” absent	1.01	0.94 to 1.09	0.79	1.22	1.02 to 1.46	0.029	0.89	0.76 to 1.05	0.17
T <sub>2</sub> W hyperintense	1.35	1.04 to 1.76	0.029	n/a	n/a	n/a	1.41	0.98 to 2.04	0.064
T <sub>1</sub> W hypointense	1.01	0.94 to 1.09	0.73	0.80	0.64 to 1.01	0.061	1.05	0.93 to 1.18	0.43
DWI hyperintense	0.94	0.80 to 1.10	0.45	n/a	n/a	n/a	0.98	0.83 to 1.16	0.82

APHE, arterial phase hyper enhancement; DPWO, delayed phase washout; DWI, diffusion weighted imaging; FS%, hepatic fat signal fraction; OR, odds ratio; PVWO, portal venous phase washout; T<sub>1</sub>W, T<sub>1</sub> weighted; T<sub>2</sub>W, T<sub>2</sub> weighted.

n/a = 100% T<sub>2</sub>W hyperintense or DWI hyperintense; Unit OR = % increase or decrease in odds of outcome for every 1% increase in hepatic FS%; data analyzed using logistic regression.

a sensitivity and specificity of 80 and 100% for absent enhancing capsule appearance (Figure 7).

## DISCUSSION

NAFLD represents a spectrum of disease ranging from NAFL to NASH ± fibrosis to NASH cirrhosis to cryptogenic cirrhosis.<sup>18</sup> NAFLD is a known risk factor for development of HCC and the HCC may arise in the absence of hepatic fibrosis or cirrhosis.<sup>2,8–17</sup> The present study sought to examine the effect of hepatic steatosis on major HCC MR imaging features in patients with both non-cirrhotic and cirrhotic, NAFLD-associated HCC. In the present cohort, 56% of HCCs occurred in the absence of cirrhotic liver morphology, similar to previous studies showing 39–49% of NAFLD-associated HCCs occurring in non-cirrhotic livers.<sup>38,39</sup> The exact prevalence and incidence of HCC in non-cirrhotic NAFLD is unknown but affects no more than 1 per 3000–4000 individuals with isolated NAFLD.<sup>40–42</sup>

Hepatic fat signal fraction (FS%) at MRI was used to quantitatively estimate hepatic steatosis. Importantly, mean hepatic FS% increased with histologic steatosis grade (mild—6.3%, moderate 11.8% and severe 21.2%), findings similar to those reported by Tang *et al* using MR imaging proton density fat fraction (PDFF) (Grade 1—6.4%, Grade 2—17.4% and Grade 3—22.1%).<sup>43</sup>

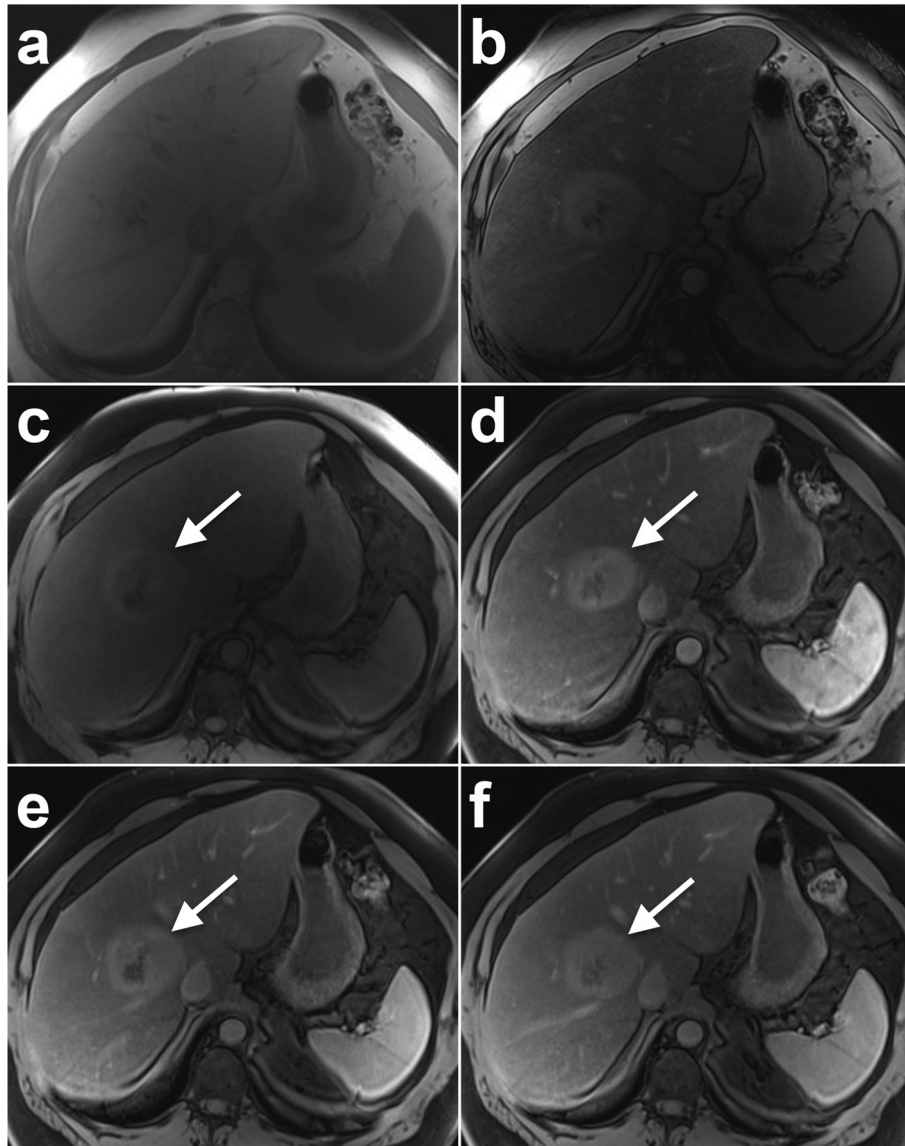
Studies on MRI features of NAFLD-associated HCC are rare. APHE is one of the CT/MRI LI-RADS® major criteria but has been reported to be absent in 10–40% of HCCs.<sup>26,28,44–49</sup> In our study, APHE was present in 45 (93%) cases overall and in agreement with current reported incidence of 86–100%.<sup>30,35</sup> Of note, absent APHE was not associated with hepatic steatosis or fibrosis/cirrhosis by MRI or pathology.

In the current study, 37% of HCCs did not show PVWO and 21% did not show DPWO, findings that are slightly higher than the 12–18% reported in earlier studies.<sup>30,35</sup> Of note, there was no difference in the proportion of HCCs showing PVWO

or DPWO between patients with cirrhotic and non-cirrhotic NAFLD. However, absent HCC washout was associated with both increasing FS% at MRI and histologic steatosis grade among patients with non-cirrhotic NAFLD. These findings may be related to the fact that increasing hepatic steatosis results in greater background liver signal loss/hypointensity on the fat-suppressed T<sub>1</sub> weighted post-contrast enhanced images, thereby resulting in the appearance of persistent HCC hyperintensity or isointensity during the portal venous and delayed phase imaging and ultimately absent washout appearance. However, given this potential masking of washout on post-contrast images due to background hepatic signal loss, digital subtraction imaging may be useful in overcoming this limitation and warrants further investigation. Additionally, prior studies have suggested small HCCs in cirrhotic livers may not demonstrate washout in up to 40–60% of cases.<sup>50,51</sup> However, in the current study tumor size was not associated with absent PVWO ( $p = 0.79$ ) or DPWO ( $p = 0.98$ ). Moreover, Jang *et al* reported differences in the timing of washout between moderate and well/poorly differentiated HCCs.<sup>52</sup> However, there was no difference in HCC PVWO ( $p = 0.81$ ) or DPWO ( $p = 0.68$ ) by histologic tumor grade in the current study.

Enhancing “capsule”, which is characteristic and relatively specific for HCC, was present in 71% of NAFLD-associated HCCs in the current study, finding slightly lower than previously reported by Iannaccone *et al* among 16 NAFLD-associated HCCs (88%).<sup>30–32</sup> Conversely, prior studies have reported a lower proportion of enhancing “capsule” (44%) in HCCs occurring in different chronic liver diseases but false-negative findings for enhancing “capsule” have been reported in up to 43% of HCCs.<sup>35,53</sup> Of note, there was no difference in the proportion of HCCs showing enhancing capsule among non-cirrhotic and cirrhotic NAFLD subgroups. However, among patients with non-cirrhotic NAFLD, absent enhancing capsule was associated with both increasing FS% at MRI and histologic steatosis grade. One hypothesis is that the fibrosis

Figure 3. A 57-year-old male with a BMI of 46 and histologically confirmed NASH and HCC. (A) In-phase and (B) opposed phase MRI images demonstrate severe steatosis (hepatic FS% = 27.8%). 6.7 cm HCC (arrow) shows (C) pre-contrast  $T_1$  weighted hyperintensity and (D) arterial phase hyperenhancement with no washout in (E) portal venous or (F) delayed phases. Note non-cirrhotic liver morphology and no features of portal hypertension. Histology showed Stage 2 fibrosis, mild active steatohepatitis and marked steatosis.

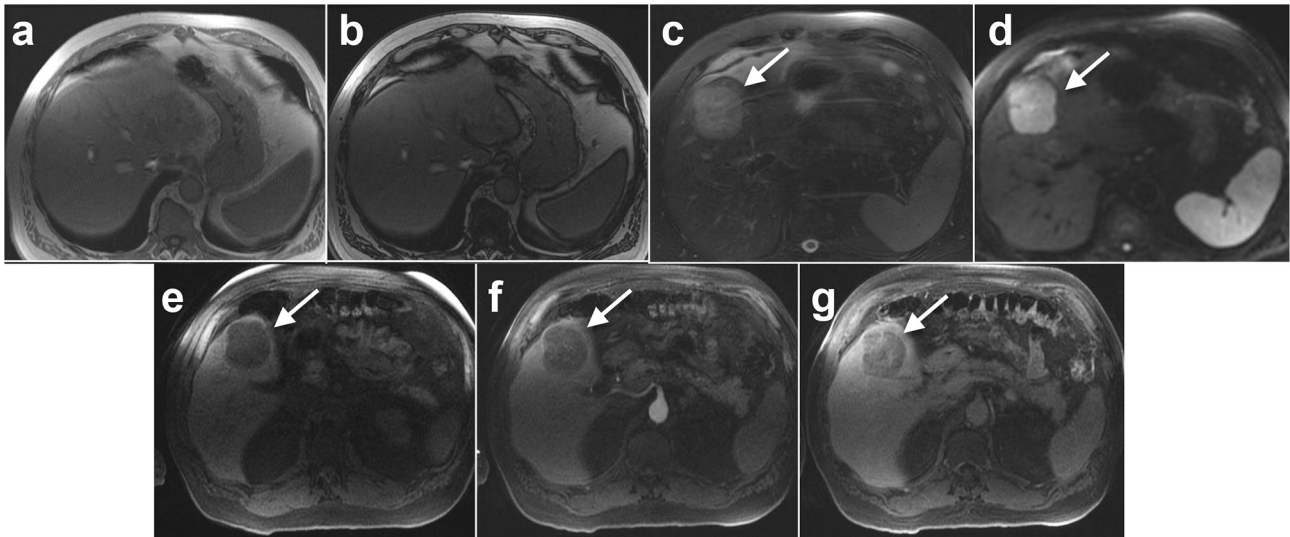


associated with cirrhosis contributes to the development of the HCC tumor capsule and subsequent enhancing “capsule” appearance. Additionally, the choice of MRI contrast medium—gadolinium-based extracellular versus hepatobiliary specific—may affect whether an enhancing capsule can be identified on later post-contrast MR images. As such, in patients with suspected or known NAFLD, gadolinium based extracellular contrast medium should be considered to optimize the ability to see an enhancing capsule.

Ancillary MRI features for HCC including intralesional fat, corona enhancement, nodule-in-nodule architecture, mosaic architecture, mild-moderate  $T_2W$  hyperintensity, restricted diffusion, lesional fat/iron sparing, transitional

or hepatobiliary phase hypointensity, and diameter increase less than threshold growth are not factored into CT/MRI LI-RADS<sup>®</sup> major criteria.<sup>32</sup> Nonetheless, mild-moderate  $T_2W$  hyperintensity is highly suggestive of malignancy if present. In the current study the majority of HCCs were  $T_2W$  hyperintense overall (88%). However, a significantly higher proportion of HCCs were  $T_2W$  hypo/isointense among patients with cirrhotic liver morphology (37%) compared to non-cirrhotic liver morphology (0%), findings similar to those reported by Hussain et al of 42–53% of HCCs being  $T_2W$  iso/hypointense in the presence of a cirrhotic liver.<sup>54</sup> As such, HCC  $T_2$  weighted hyperintensity may be more common in non-cirrhotic NAFLD-associated HCC. Diffusion restriction is highly suggestive of malignancy if present and was observed in the

Figure 4. A 66-year-old male with a BMI of 32 and histologically confirmed NAFL and HCC. (A) In-phase and (B) opposed phase MRI images demonstrate minimal to no steatosis (hepatic FS% = 3.3%). 5.6 cm HCC (arrow) shows (C)  $T_2$  weighted hyperintensity, (D) diffusion hyperintensity and (E)  $T_1$  weighted hypointensity. Contrast-enhanced imaging shows (F) no arterial phase hyperenhancement but (G) slight enhancement during delayed phase imaging. Note non-cirrhotic liver morphology and no features of portal hypertension. Histology showed stage 0 fibrosis and mild steatosis but not steatohepatitis.



majority of cases (88%), similar to 84% in an earlier study.<sup>55</sup> Of note, DWI hyperintensity was more common in patients without cirrhosis (100%) than with cirrhosis (69%). As such,

DWI may be particularly important ancillary feature in cases of non-cirrhotic NAFLD associated HCC that do not demonstrate washout.

Figure 5. An 83 year old male with a BMI of 29 and diabetes was initially presumed to have cryptogenic cirrhosis but later histologically confirmed NASH and HCC. (A) In-phase and (B) opposed phase MRI images demonstrate no steatosis (hepatic FS% = 1.7%). A 4.0 cm HCC in segment VII/VIII (arrow) shows (C) mild  $T_2$  weighted hyperintensity. Contrast-enhanced imaging shows (D) pre-contrast  $T_1$  weighted isointensity, (E) mild arterial phase hyperenhancement, (F) portal venous phase isointensity without washout and (G) delayed phased washout with enhancing capsule appearance. Note cirrhotic liver morphology and features of portal hypertension including splenomegaly, ascites and upper abdominal venous collaterals. (H) Gross pathology image shows a heterogeneous pale-tan mass with a thin peripheral fibrous capsule and background hepatic macroscopic steatosis. Histology showed Stage 4 fibrosis, mild focal steatosis and mildly active steatohepatitis.

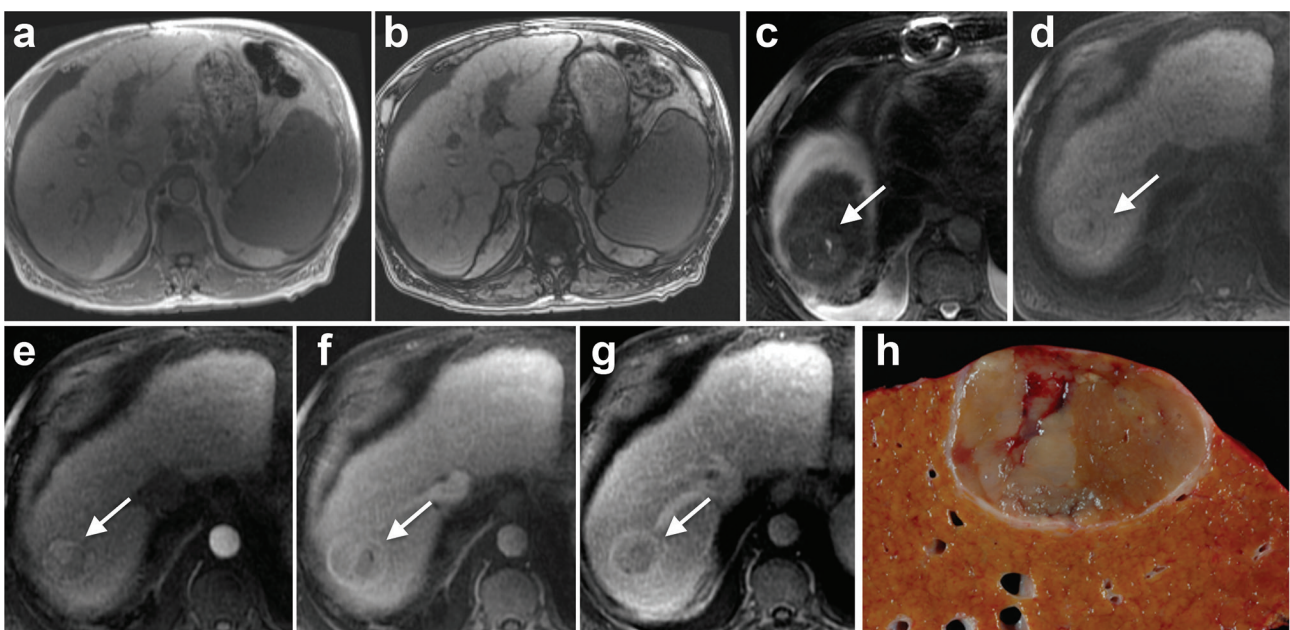
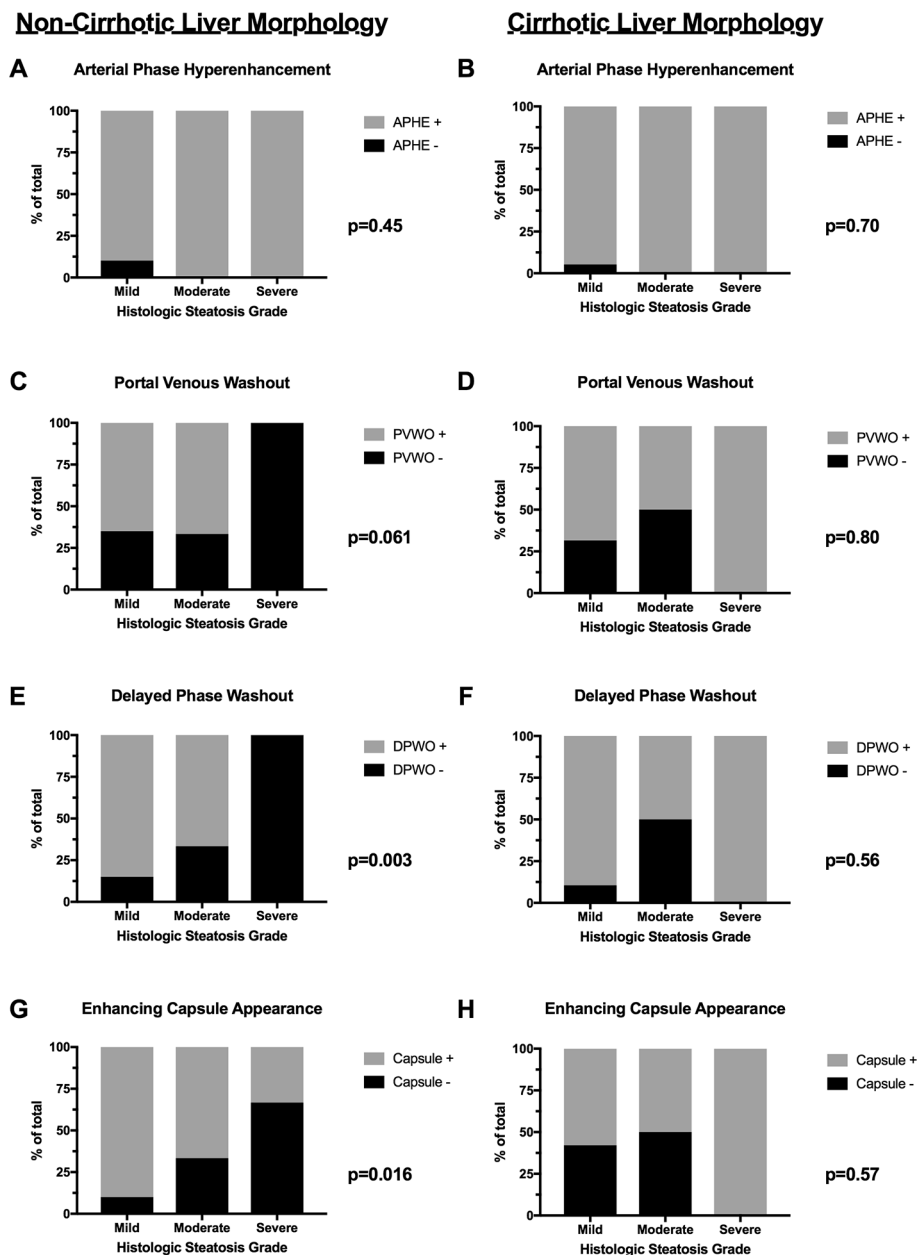




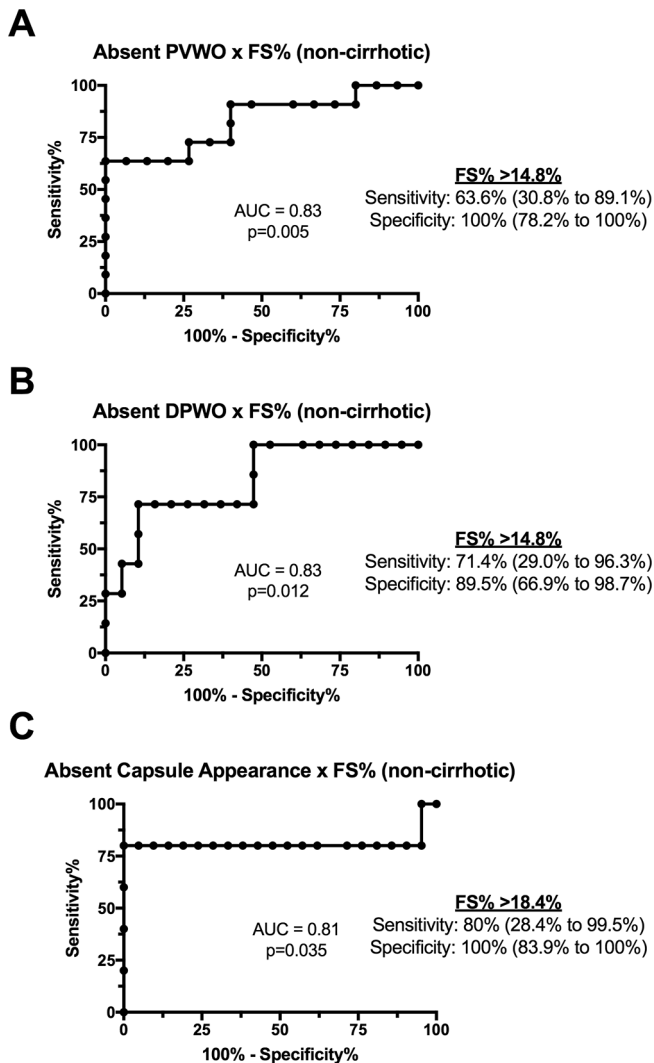
Figure 6. HCC major features by histologic steatosis grade in patients with NAFLD-associated HCC stratified by liver morphology at MRI. Percentage of HCCs with absent (A, B) arterial phase hyperenhancement (APHE), (C, D) portal venous phase washout (PVWO), (E-F) delayed phased washout (DPWO) or (G-H) enhancing “capsule” appearance by mild, moderate or severe histologic steatosis grade among patients with (A, C, E, G) non-cirrhotic liver morphology or (B, D, F, H) cirrhotic liver morphology.



Interestingly, there were no significant differences in major HCC imaging features in patients with non-cirrhotic versus cirrhotic NAFLD. However, absent washout and enhancing capsule appearance were associated with increasing steatosis among patients with non-cirrhotic NAFLD. Taken together, these findings suggest that imaging appearance of NAFLD-associated HCC may vary significantly along the NAFLD disease spectrum depending on the degree of hepatic steatosis and presence of cirrhosis and further studies are needed to better define the imaging appearance of NAFLD-associated HCC as well as compare with non-NAFLD associated HCC.

While prior studies have examined interobserver agreement for HCC major features in cirrhotics, interobserver agreement has not yet been explored in the setting of NAFLD.<sup>33-35</sup> In chronic liver diseases of other etiologies, good agreement for APHE and washout and moderate agreement for enhancing “capsule” were reported.<sup>35</sup> In the current study similar findings were observed with good agreement for APHE among all readers and fair to good agreement for enhancing “capsule”. However, there was greater variability in agreement for washout with fair to moderate agreement for PVWO and moderate to good for DPWO. Given the higher proportion of HCCs demonstrating DPWO and the greater agreement for washout during delayed phase imaging,

Figure 7. Receiver operating characteristic (ROC) curves for differentiating (A) portal venous washout (PVWO), (B) delayed phase washout (DPWO) and (C) enhancing capsule appearance by hepatic fat signal fraction (FS%) in 26 patients with non-cirrhotic NAFLD-associated HCC.



delayed phase imaging should be routinely performed in patients with NAFLD undergoing contrast-enhanced MRI. Additionally, inter-rater agreement was moderate to good for assessment of cirrhotic liver morphology.

There are limitations to this study. This was a retrospective review of 48 patients over a relatively long time period—15 years.

We did not include NAFLD patients with an imaging diagnosis of HCC but with no histological confirmation, which would have yielded a larger cohort. However, the inclusion of cases of HCC diagnosed by imaging alone would capture only patients who had major features present and exclude those that did not meet the diagnosis criteria but still may have had HCC. Future studies should seek to determine the comparative imaging features between NAFLD and non-NAFLD associated HCC as well as HCC in the setting of co-morbid hepatic steatosis and other chronic liver diseases. Furthermore, due to the long time period and retrospective nature of this study, the MRI technique including scanner, field strength (1.5 T vs 3.0T), sequence protocol(s) and contrast agent(s) was not uniform across all patients. Next, hepatic FS% was used to quantitatively measure hepatic steatosis. There are known limitations to this method.<sup>36</sup> Nonetheless, hepatic FS% is less subject to changes in MRI technique over time given the ratio of fat fraction rather than absolute fat quantification. Future studies of NAFLD-associated HCC should consider additional techniques for quantitatively measuring hepatic fat content at MRI such as PDFF.<sup>36</sup> Lastly, ultrasound is currently recommended for screening patients at risk for HCC but may have decreased sensitivity for detecting liver masses in the setting of diffuse hepatic steatosis. As such, multicenter prospective, longitudinal imaging studies in patients with NAFLD are needed not only to determine the best approach to screening this population for HCC but also to develop standardized imaging protocols and highly specific criteria for non-invasive imaging diagnosis of NAFLD-associated HCC, particularly in the setting of transplant allocation.

The present findings suggest that in patients with NAFLD-associated HCC, >50% of HCCs may occur in the absence of cirrhotic liver morphology. Moreover, in non-cirrhotic, NAFLD-associated HCC, absent HCC washout and capsule appearance are associated with increasing hepatic steatosis, thereby potentially impacting the noninvasive imaging diagnosis of HCC in these patients. In fact, LI-RADS<sup>®</sup>, EASL-EORTC and AASLD guidelines for non-invasive diagnosis of HCC have not been validated in patients with NAFLD in whom imaging evidence of cirrhosis may be absent. Imaging criteria for HCC diagnosis in patients with non-cirrhotic NAFLD are particularly of interest as these liver masses are not eligible for LI-RADS categorization or EASL-EORTC and AASLD criteria.<sup>23,24,28,29</sup> In short, absent washout and capsule appearance in non-cirrhotic NAFLD may require alternative criteria for the diagnosis of HCC in these patients.

## REFERENCES

1. Ferlay J, Soerjomataram I, Dikshit R, Eser S, Mathers C, Rebelo M, et al. Cancer incidence and mortality worldwide: sources, methods and major patterns in GLOBOCAN 2012. *Int J Cancer* 2015; **136**: E359–E386. doi: <https://doi.org/10.1002/ijc.29210>
2. Yang JD, Kim B, Sanderson SO, St Sauver JL, Yawn BP, Pedersen RA, et al. Hepatocellular carcinoma in olmsted county, Minnesota, 1976–2008. *Mayo Clin Proc* 2012; **87**: 9–16. doi: <https://doi.org/10.1016/j.mayocp.2011.07.001>
3. Yang JD, Ahmed Mohammed H, Harmsen WS, Enders F, Gores GJ, Roberts LR.

- Recent trends in the epidemiology of hepatocellular carcinoma in Olmsted county, Minnesota: a US population-based study. *J Clin Gastroenterol* 2017; **51**: 742–. doi: <https://doi.org/10.1097/MCG.0000000000000810>
4. Llovet JM, Zucman-Rossi J, Pikarsky E, Sangro B, Schwartz M, Sherman M, et al. Hepatocellular carcinoma. *Nat Rev Dis Primers* 2016; **2**: 16018. doi: <https://doi.org/10.1038/nrdp.2016.18>
  5. Tsukuma H, Hiyama T, Tanaka S, Nakao M, Yabuuchi T, Kitamura T, et al. Risk factors for hepatocellular carcinoma among patients with chronic liver disease. *N Engl J Med* 1993; **328**: 1797–801. doi: <https://doi.org/10.1056/NEJM199306243282501>
  6. Yang JD, Kim WR, Coelho R, Mettler TA, Benson JT, Sanderson SO, Therneau TM, et al. Cirrhosis is present in most patients with hepatitis B and hepatocellular carcinoma. *Clin Gastroenterol Hepatol* 2011; **9**: 64–70. doi: <https://doi.org/10.1016/j.cgh.2010.08.019>
  7. Shire AM, Sandhu DS, Kaiya JK, Oseini AM, Yang JD, Chaiteerakij R, et al. Viral hepatitis among Somali immigrants in Minnesota: association of hepatitis C with hepatocellular carcinoma. *Mayo Clin Proc* 2012; **87**: 17–24. doi: <https://doi.org/10.1016/j.mayocp.2011.08.001>
  8. White DL, Kanwal F, El-Serag HB. Association between nonalcoholic fatty liver disease and risk for hepatocellular cancer, based on systematic review. *Clin Gastroenterol Hepatol* 2012; **10**: 1342–59. doi: <https://doi.org/10.1016/j.cgh.2012.10.001>
  9. Michelotti GA, Machado MV, Diehl AM. NAFLD, NASH and liver cancer. *Nat Rev Gastroenterol Hepatol* 2013; **10**: 656–65. doi: <https://doi.org/10.1038/nrgastro.2013.183>
  10. Marrero JA, Fontana RJ, Su GL, Conjeevaram HS, Emick DM, Lok AS. NAFLD may be a common underlying liver disease in patients with hepatocellular carcinoma in the United States. *Hepatology* 2002; **36**: 1349–54. doi: <https://doi.org/10.1002/hep.1840360609>
  11. Guzman G, Brunt EM, Petrovic LM, Chejfec G, Layden TJ, Cotler SJ. Does nonalcoholic fatty liver disease predispose patients to hepatocellular carcinoma in the absence of cirrhosis? *Arch Pathol Lab Med* 2008; **132**: 1761–6. doi: <https://doi.org/10.1043/1543-2165-132.11.1761>
  12. Malik SM, Gupta PA, de Vera ME, Ahmad J. Liver transplantation in patients with nonalcoholic steatohepatitis-related hepatocellular carcinoma. *Clin Gastroenterol Hepatol* 2009; **7**: 800–6. doi: <https://doi.org/10.1016/j.cgh.2009.02.025>
  13. Huckle F, Sieghart W, Schöniger-Hekele M, Peck-Radosavljevic M, Müller C. Clinical characteristics of patients with hepatocellular carcinoma in Austria - is there a need for a structured screening program? *Wien Klin Wochenschr* 2011; **123**: 542–51. doi: <https://doi.org/10.1007/s00508-011-0033-9>
  14. Ertle J, Dechêne A, Sowa JP, Penndorf V, Herzer K, Kaiser G, et al. Non-alcoholic fatty liver disease progresses to hepatocellular carcinoma in the absence of apparent cirrhosis. *Int J Cancer* 2011; **128**: 2436–43. doi: <https://doi.org/10.1002/ijc.25797>
  15. Gonçalves PL, Zago-Gomes MP, Marques CC, Mendonça AT, Gonçalves CS, Pereira FE. Etiology of liver cirrhosis in Brazil: chronic alcoholism and hepatitis viruses in liver cirrhosis diagnosed in the state of Espírito Santo. *Clinics* 2013; **68**: 291–5. doi: [https://doi.org/10.6061/clinics/2013\(03\)OA02](https://doi.org/10.6061/clinics/2013(03)OA02)
  16. Margini C, Dufour JF. The story of HCC in NAFLD: from epidemiology, across pathogenesis, to prevention and treatment. *Liver Int* 2016; **36**: 317–24. doi: <https://doi.org/10.1111/liv.13031>
  17. Perumpail RB, Wong RJ, Ahmed A, Harrison SA. Hepatocellular carcinoma in the setting of non-cirrhotic nonalcoholic fatty liver disease and the metabolic syndrome: US experience. *Dig Dis Sci* 2015; **60**: 3142–8. doi: <https://doi.org/10.1007/s10620-015-3821-7>
  18. Chalasani N, Younossi Z, Lavine JE, Charlton M, Cusi K, Rinella M, et al. The diagnosis and management of nonalcoholic fatty liver disease: practice guidance from the American association for the study of liver diseases. *Hepatology* 2018; **67**: 328–57. doi: <https://doi.org/10.1002/hep.29367>
  19. Tilg H, Moschen AR, Roden M. NAFLD and diabetes mellitus. *Nat Rev Gastroenterol Hepatol* 2017; **14**: 32–42. doi: <https://doi.org/10.1038/nrgastro.2016.147>
  20. Siegel AB, Zhu AX. Metabolic syndrome and hepatocellular carcinoma: two growing epidemics with a potential link. *Cancer* 2009; **115**: 5651–61. doi: <https://doi.org/10.1002/cncr.24687>
  21. Lazo M, Hernaez R, Eberhardt MS, Bonekamp S, Kamel I, Guallar E, et al. Prevalence of nonalcoholic fatty liver disease in the United States: the Third National Health and Nutrition Examination Survey, 1988–1994. *Am J Epidemiol* 2013; **178**: 38–45. doi: <https://doi.org/10.1093/aje/kws448>
  22. Sherif ZA, Saeed A, Ghavimi S, Nouraie SM, Laiyemo AO, Brim H, et al. Global epidemiology of nonalcoholic fatty liver disease and perspectives on us minority populations. *Dig Dis Sci* 2016; **61**: 1214–25. doi: <https://doi.org/10.1007/s10620-016-4143-0>
  23. European Association For The Study Of The Liver, European Organisation For Research And Treatment Of Cancer EASL-EORTC clinical practice guidelines: management of hepatocellular carcinoma. *J Hepatol* 2012; **56**: 908–43. doi: <https://doi.org/10.1016/j.jhep.2011.12.001>
  24. Bruix J, Sherman M. American association for the study of liver D. Management of hepatocellular carcinoma: an update. *Hepatology* 2011; **53**: 1020–2.
  25. Venkatesh SK, Chandan V, Roberts LR. Liver masses: a clinical, radiologic, and pathologic perspective. *Clin Gastroenterol Hepatol* 2014; **12**: 1414–29. doi: <https://doi.org/10.1016/j.cgh.2013.09.017>
  26. Mitchell DG, Bruix J, Sherman M, Sirlin CB. LI-RADS (Liver Imaging Reporting and Data System): summary, discussion, and consensus of the LI-RADS Management Working Group and future directions. *Hepatology* 2015; **61**: 1056–65. doi: <https://doi.org/10.1002/hep.27304>
  27. Leoni S, Piscaglia F, Golfieri R, Camaggi V, Vidili G, Pini P, et al. The impact of vascular and nonvascular findings on the noninvasive diagnosis of small hepatocellular carcinoma based on the EASL and AASLD criteria. *Am J Gastroenterol* 2010; **105**: 599–609. doi: <https://doi.org/10.1038/ajg.2009.654>
  28. American College of Radiology. Liver imaging reporting and data system version. 2014. Available from: <http://www.acr.org/Quality-Safety/Resources/LIRADS> [Accessed April 28, 2017].
  29. American College of Radiology. Liver imaging reporting and data system version. 2017. Available from: <https://www.acr.org/Quality-Safety/Resources/LIRADS/LIRADS-v2017> [Accessed June 28, 2018].
  30. Iannaccone R, Piacentini F, Murakami T, Paradis V, Belghiti J, Hori M, et al. Hepatocellular carcinoma in patients with nonalcoholic fatty liver disease: helical CT and MR imaging findings with clinical-pathologic comparison. *Radiology* 2007; **243**: 422–30. doi: <https://doi.org/10.1148/radiol.2432051244>
  31. Choi JY, Lee JM, Sirlin CB. CT and MR imaging diagnosis and staging of hepatocellular carcinoma: part I. Development, growth, and spread: key pathologic and imaging aspects. *Radiology* 2014; **272**: 635–54. doi: <https://doi.org/10.1148/radiol.14132361>
  32. Choi JY, Lee JM, Sirlin CB. CT and MR imaging diagnosis and staging of hepatocellular carcinoma: part II. Extracellular agents, hepatobiliary agents,

- and ancillary imaging features. *Radiology* 2014; **273**: 30–50. doi: <https://doi.org/10.1148/radiol.14132362>
33. Davenport MS, Khalatbari S, Liu PS, Maturen KE, Kaza RK, Wasnik AP, et al. Repeatability of diagnostic features and scoring systems for hepatocellular carcinoma by using MR imaging. *Radiology* 2014; **272**: 132–42. doi: <https://doi.org/10.1148/radiol.14131963>
  34. Ehman EC, Umetsu SE, Ohliger MA, Fidelman N, Ferrell LD, Yeh BM, et al. Imaging prediction of residual hepatocellular carcinoma after locoregional therapy in patients undergoing liver transplantation or partial hepatectomy. *Abdom Radiol* 2016; **41**: 2161–8. doi: <https://doi.org/10.1007/s00261-016-0837-1>
  35. Ehman EC, Behr SC, Umetsu SE, Fidelman N, Yeh BM, Ferrell LD, et al. Rate of observation and inter-observer agreement for LI-RADS major features at CT and MRI in 184 pathology proven hepatocellular carcinomas. *Abdom Radiol* 2016; **41**: 963–9. doi: <https://doi.org/10.1007/s00261-015-0623-5>
  36. Reeder SB, Cruite I, Hamilton G, Sirlin CB. Quantitative assessment of liver fat with magnetic resonance imaging and spectroscopy. *J Magn Reson Imaging* 2011; **34**: 729–49. doi: <https://doi.org/10.1002/jmri.22580>
  37. Byrt T, Bishop J, Carlin JB, Bias CJB. Bias, prevalence and kappa. *J Clin Epidemiol* 1993; **46**: 423–9. doi: [https://doi.org/10.1016/0895-4356\(93\)90018-V](https://doi.org/10.1016/0895-4356(93)90018-V)
  38. Baffy G, Brunt EM, Caldwell SH. Hepatocellular carcinoma in non-alcoholic fatty liver disease: an emerging menace. *J Hepatol* 2012; **56**: 1384–91. doi: <https://doi.org/10.1016/j.jhep.2011.10.027>
  39. Yasui K, Hashimoto E, Komorizono Y, Koike K, Arai S, Imai Y, et al. Characteristics of patients with nonalcoholic steatohepatitis who develop hepatocellular carcinoma. *Clin Gastroenterol Hepatol* 2011; **9**: 428–33. doi: <https://doi.org/10.1016/j.cgh.2011.01.023>
  40. Baffy G. Hepatocellular Carcinoma in Non-alcoholic Fatty Liver Disease: Epidemiology, Pathogenesis, and Prevention. *J Clin Transl Hepatol* 2013; **1**: 131–7. doi: <https://doi.org/10.14218/JCTH.2013.00005>
  41. Ekstedt M, Franzén LE, Mathiesen UL, Thorelius L, Holmqvist M, Bodemar G, et al. Long-term follow-up of patients with NAFLD and elevated liver enzymes. *Hepatology* 2006; **44**: 865–73. doi: <https://doi.org/10.1002/hep.21327>
  42. Rafiq N, Bai C, Fang Y, Srishord M, McCullough A, Gramlich T, et al. Long-term follow-up of patients with nonalcoholic fatty liver. *Clin Gastroenterol Hepatol* 2009; **7**: 234–8. doi: <https://doi.org/10.1016/j.cgh.2008.11.005>
  43. Tang A, Desai A, Hamilton G, Wolfson T, Gamst A, Lam J, et al. Accuracy of MR imaging-estimated proton density fat fraction for classification of dichotomized histologic steatosis grades in nonalcoholic fatty liver disease. *Radiology* 2015; **274**: 416–25. doi: <https://doi.org/10.1148/radiol.14140754>
  44. Llovet JM, Bustamante J, Castells A, Vilana R, Ayuso MC, Sala M, et al. Natural history of untreated nonsurgical hepatocellular carcinoma: rationale for the design and evaluation of therapeutic trials. *Hepatology* 1999; **29**: 62–7. doi: <https://doi.org/10.1002/hep.510290145>
  45. Hanna RF, Aguirre DA, Kased N, Emery SC, Peterson MR, Sirlin CB. Cirrhosis-associated hepatocellular nodules: correlation of histopathologic and MR imaging features. *Radiographics* 2008; **28**: 747–69. doi: <https://doi.org/10.1148/rg.283055108>
  46. Rosenkrantz AB, Lee L, Matza BW, Kim S. Infiltrative hepatocellular carcinoma: comparison of MRI sequences for lesion conspicuity. *Clin Radiol* 2012; **67**: e105–e111. doi: <https://doi.org/10.1016/j.crad.2012.08.019>
  47. Sano K, Ichikawa T, Motosugi U, Sou H, Muhi AM, Matsuda M, et al. Imaging study of early hepatocellular carcinoma: usefulness of gadoxetic acid-enhanced MR imaging. *Radiology* 2011; **261**: 834–44. doi: <https://doi.org/10.1148/radiol.11101840>
  48. Kim SH, Lee WJ, Lim HK, Park CK. SPIO-enhanced MRI findings of well-differentiated hepatocellular carcinomas: correlation with MDCT findings. *Korean J Radiol* 2009; **10**: 112–20. doi: <https://doi.org/10.3348/kjr.2009.10.2.112>
  49. Kanematsu M, Semelka RC, Leonardou P, Mastropasqua M, Lee JK. Hepatocellular carcinoma of diffuse type: MR imaging findings and clinical manifestations. *J Magn Reson Imaging* 2003; **18**: 189–95. doi: <https://doi.org/10.1002/jmri.10336>
  50. Sangiovanni A, Manini MA, Iavarone M, Romeo R, Forzenigo LV, Fraquelli M, et al. The diagnostic and economic impact of contrast imaging techniques in the diagnosis of small hepatocellular carcinoma in cirrhosis. *Gut* 2010; **59**: 638–44. doi: <https://doi.org/10.1136/gut.2009.187286>
  51. Khan AS, Hussain HK, Johnson TD, Weadock WJ, Pelletier SJ, Marrero JA. Value of delayed hypointensity and delayed enhancing rim in magnetic resonance imaging diagnosis of small hepatocellular carcinoma in the cirrhotic liver. *J Magn Reson Imaging* 2010; **32**: 360–6. doi: <https://doi.org/10.1002/jmri.22271>
  52. Jang HJ, Kim TK, Burns PN, Wilson SR. Enhancement patterns of hepatocellular carcinoma at contrast-enhanced US: comparison with histologic differentiation. *Radiology* 2007; **244**: 898–906. doi: <https://doi.org/10.1148/radiol.2443061520>
  53. Zhang YD, Zhu FP, Xu X, Wang Q, Wu CJ, Liu XS, et al. Liver Imaging Reporting and Data System:: Substantial Discordance Between CT and MR for Imaging Classification of Hepatic Nodules. *Acad Radiol* 2016; **23**: 344–52. doi: <https://doi.org/10.1016/j.acra.2015.11.002>
  54. Hussain HK, Syed I, Nghiem HV, Johnson TD, Carlos RC, Weadock WJ, et al. T2-weighted MR imaging in the assessment of cirrhotic liver. *Radiology* 2004; **230**: 637–44. doi: <https://doi.org/10.1148/radiol.2303020921>
  55. Lee MH, Kim SH, Park MJ, Park CK, Rhim H. Gadoteric acid-enhanced hepatobiliary phase MRI and high-b-value diffusion-weighted imaging to distinguish well-differentiated hepatocellular carcinomas from benign nodules in patients with chronic liver disease. *AJR Am J Roentgenol* 2011; **197**: W868–W875. doi: <https://doi.org/10.2214/AJR.10.6237>